

Site and Oxidation-State Specificity Yielding Dimensional Control in Perovskite Ruthenates

Job T. Rijssenbeek,[†] Sylvie Malo,[‡] Vincent Caignaert,[‡] and Kenneth R. Poeppelmeier^{*,†}

Department of Chemistry, Northwestern University, 2145 Sheridan Road, Evanston, Illinois 60208-3113, and Laboratoire CRISMAT-ISMRA, Université de Caen, 6 Boulevard du Maréchal Juin, 14050 Caen, Cedex, France

Received November 21, 2001

In this communication we report the synthesis and structural characterization of the first ruthenium-based 2:1 ordered perovskite, $\text{Sr}_3\text{CaRu}_2\text{O}_9$. Ruthenium's unusual ability to readily adopt both IV(d^4) and V(d^3) oxidation states, when prepared in air, endows ruthenates with a host of different possible structures. The magnetic and electronic properties elicited by these many structural motifs have been equally diverse. For example, SrRuO_3 is a ferromagnetic metal¹ whereas CaRuO_3 is paramagnetic at all temperatures,² although ferromagnetism may be induced by transition-metal substitution.³ Sr_2RuO_4 is the only example of a layered noncuprate oxide superconductor⁴ and $\text{GdSr}_2\text{RuCu}_2\text{O}_8$ shows the microscopic coexistence of magnetic order and superconductivity.^{5,6} These fascinating properties, which undoubtedly arise from the large degree of hybridization between oxygen p-orbitals and the extended ruthenium 4d-orbitals, once again focus attention on the synthesis of new materials and the interplay between stoichiometry and structure.

The structure of $\text{Sr}_3\text{CaRu}_2\text{O}_9$, or $\text{Sr}(\text{Ca}_{1/3}\text{Ru}_{2/3})\text{O}_3$, is characterized by a 2:1 ordering of Ru^{5+} and Ca^{2+} over the six-coordinate B-sites of the perovskite lattice (Figure 1). Similarly ordered materials based on Nb^{5+} or Ta^{5+} are known and serve as good dielectrics for microwave applications.⁷ In the latter, the majority octahedral cation shifts slightly toward one face of its octahedron. Consequently, this type of ordering has only been observed when the majority site is occupied by a d^0 cation (e.g., Nb^{5+} , Ta^{5+} , etc.). To our knowledge, $\text{Sr}_3\text{CaRu}_2\text{O}_9$ is the first reported example of this structure type based on a majority metal with d electrons.

$\text{Sr}_3\text{CaRu}_2\text{O}_9$ was synthesized by solid-state reaction of stoichiometric amounts of the alkali earth carbonates (99.99%) and dried RuO_2 (99.95%). The reactants were ground and calcined for 12 h at 850 °C in air. Additional cycles of grinding and heating to 1200 °C were carried out until phase purity was achieved as determined by powder X-ray diffraction (PXRD).

Excluding several weak peaks ($I/I_{\text{max}} < 0.02$), the PXRD pattern of $\text{Sr}_3\text{CaRu}_2\text{O}_9$ could be modeled by a 2:1 ordered perovskite framework with untitled octahedra⁸ using the trigonal space group $P-3m1$ with $a = b = 5.69$ Å and $c = 7.02$ Å. The presence of unindexed peaks suggested the existence of a supercell. A subsequent electron diffraction study confirmed the presence of a monoclinic unit cell with $a \approx 17$ Å, $b \approx 5.6$ Å, $c \approx 9.6$ Å and $\beta \approx 125^\circ$. The extinction conditions were compatible with space group $P2_1/c$. All peaks in the PXRD pattern could be indexed using this unit cell. Energy-dispersive X-ray analysis performed on numerous crystallites confirmed the Sr:Ca:Ru ratios to be 3.01:1.02:1.97. Hydrogen reduction thermogravimetric analysis indicated a weight loss of 12.29% consistent with an oxygen stoichiometry of nine (calculated weight loss 12.33%). For the structure determination, neutron diffraction data were collected on

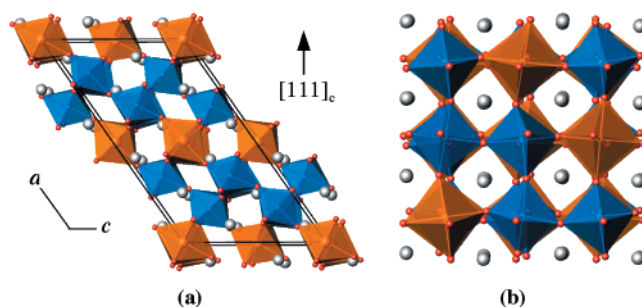


Figure 1. Structure of $\text{Sr}_3\text{CaRu}_2\text{O}_9$ viewed along the [010] direction (a) and along one of the pseudocubic axes (b). RuO_6 octahedra are blue, CaO_6 octahedra are orange, and Sr atoms are gray. The cubic [111] direction, perpendicular to the close-packed planes, is shown.

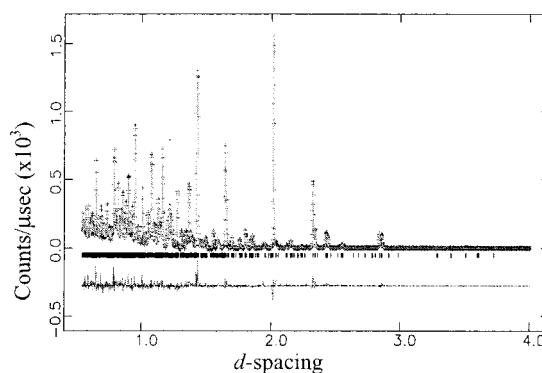


Figure 2. Observed (crosses), calculated (line) and difference (bottom line) neutron diffraction pattern of polycrystalline $\text{Sr}_3\text{CaRu}_2\text{O}_9$. Allowed Bragg reflections are marked (vertical bars).

a polycrystalline sample. The atomic positions used for the initial structural model were derived from the $P-3m1$ subcell. The model refined well in $P2_1/c$ with lattice parameters $a = 17.1540(5)$ Å, $b = 5.6891(2)$ Å, $c = 9.8627(3)$ Å, $\beta = 125.0(1)^\circ$ and $Z = 4$ (Figure 2).⁹

$\text{Sr}_3\text{CaRu}_2\text{O}_9$ consists of corner-connected RuO_6 and CaO_6 octahedra sequenced $\{\dots\text{Ru}\text{--}\text{Ru}\text{--}\text{Ca}\dots\}$ along each of the pseudocubic directions of perovskite (Figure 1b). Equivalently, owing to the ordering of the B-site cations, the structure can be viewed¹⁰ as layered parallel to the close-packed planes (i.e., the (111) planes of cubic perovskite) with one layer of CaO_6 octahedra alternating with two layers of RuO_6 octahedra (Figure 1a). The 2:1 cation ordering over the octahedral sites is due to the size and charge differences between ruthenium and calcium.

The sizable mismatch between Ru—O (1.97 Å) and Ca—O (2.4 Å) bond-lengths leads to significant tilting, twisting and deformation of the octahedra. The bond lengths reveal that while the two crystallographically distinct CaO_6 octahedra are under compression they remain relatively undistorted (standard deviation in bond lengths, $\sigma_{\text{BL}} = 0.012, 0.007$). In contrast, the two distinct RuO_6

* To whom correspondence should be addressed.

[†] Northwestern University.

[‡] Université de Caen.

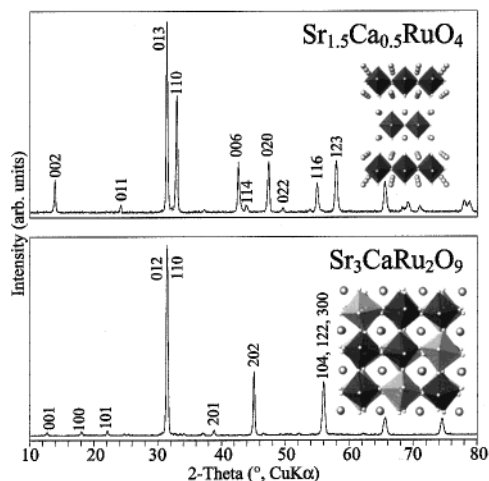


Figure 3. Top: X-ray diffractogram of polycrystalline $\text{Sr}_{1.5}\text{Ca}_{0.5}\text{RuO}_4$ synthesized by reduction of $\text{Sr}_3\text{CaRu}_2\text{O}_9$. Bottom: Diffraction pattern of polycrystalline $\text{Sr}_3\text{CaRu}_2\text{O}_9$ prepared by oxidation of $\text{Sr}_{1.5}\text{Ca}_{0.5}\text{RuO}_4$. For clarity, peaks in the $\text{Sr}_3\text{CaRu}_2\text{O}_9$ pattern are indexed based on the $P-3m1$ subcell.

octahedra are under slight tension and more distorted ($\sigma_{\text{BL}} = 0.113, 0.042$). In the absence of cation ordering, the tilting may be described as $a^+b^-b^-$ using Glazer's notation.¹¹ This tilt system, when combined with the 2:1 cation ordering, is consistent with the selection of $P2_1/c$ as the space group.¹² Although Ca^{2+} and Ru^{5+} are expected to have close to regular octahedral coordination, such distortions are also observed in $\text{Ca}_3\text{CaNb}_2\text{O}_9$.¹³

$\text{Sr}_3\text{CaRu}_2\text{O}_9$ and $\text{Ca}_3\text{CaNb}_2\text{O}_9$ are strikingly similar. In each case, the atom connectivity and the B-site ordering vector, perpendicular to the AO_3 close-packed planes, are the same. Both share the same tilt pattern, space group and lattice parameters, however the a and c axes are switched. The altered orientation produces a subtle structural change owing to the different orientation of the c -glide. As represented in Figure 1a, the glide in $\text{Sr}_3\text{CaRu}_2\text{O}_9$ lies in the c direction, whereas in $\text{Ca}_3\text{CaNb}_2\text{O}_9$ it is along the a direction. Levin et al. have anticipated this possibility in their description of $\text{Ca}_3\text{CaNb}_2\text{O}_9$, although it was not observed in that system.¹³

The formation of three-dimensional (3D) $\text{Sr}_3\text{CaRu}_2\text{O}_9$ is remarkable considering the existence of the two-dimensional (2D) $\text{Sr}_{1.5}\text{Ca}_{0.5}\text{RuO}_4$ (i.e., $\text{Sr}_3\text{CaRu}_2\text{O}_8$)¹⁴ with the same ratio of cations and the pseudo-one-dimensional $\text{Sr}_4\text{Ru}_2\text{O}_9$.¹⁵ Perhaps it is not surprising, then, that both were often encountered as secondary phases during intermediate reaction steps. $\text{Sr}_{1.5}\text{Ca}_{0.5}\text{RuO}_4$ is metallic and adopts a layered $n = 1$ Ruddlesden–Popper structure, wherein the Ca^{2+} and Sr^{2+} occupy the nine-coordinate A-sites between isolated $\text{RuO}_4/2\text{O}_2$ slabs.¹⁴ Although structurally very different, $\text{Sr}_{1.5}\text{Ca}_{0.5}\text{RuO}_4$ and $\text{Sr}_3\text{CaRu}_2\text{O}_9$ have stoichiometries that differ only in their oxygen content. To elucidate the effect of the oxygen content and the ruthenium valence, experiments were undertaken in argon, air, and oxygen. $\text{Sr}_3\text{CaRu}_2\text{O}_9$, initially synthesized in air, was quantitatively converted to $\text{Sr}_{1.5}\text{Ca}_{0.5}\text{RuO}_4$ by treatment in 1 atm flowing argon for 24 h at 1200 °C. Reoxidation returns the original 3D structure after 24 h at 1000 °C in 1 atm flowing oxygen (Figure 3). This transformation can be repeated multiple times with the same result. Temperature-dependent resistivity measurements indicated $\text{Sr}_3\text{CaRu}_2\text{O}_9$ is semiconducting ($\rho_{100\text{K}}/\rho_{300\text{K}} = 17.8$). Thus, by controlling the synthesis conditions, structures of different dimensionalities and properties result.

This structural transformation is made possible by the unique combination of the oxidation state of ruthenium and the coordination of calcium. First, ruthenium's two available oxidation states allow two oxygen stoichiometries yielding two different structures.

Second, calcium, which can occupy six-, nine- and twelve-coordinate sites, is essential for the formation of a 3D perovskite structure. Larger cations would not fit into the octahedral sites of the perovskite structure and would yield structures related to $\text{Sr}_4\text{Ru}_2\text{O}_9$ or multiphase products.

The Sr–Ca–Ru–O system provides a significant opportunity with respect to thin-film fabrication of metal–insulator–metal (MIM) or metal–insulator–semiconductor (MIS) devices. Using a single precursor composition the properties of a deposited film could be regulated solely by the oxygen partial pressure.

$\text{Sr}_3\text{CaRu}_2\text{O}_9$ is the first example of a 2:1 ordered perovskite with a non- d^0 majority metal. Previous examples had been limited to metals such as Nb^{5+} , Ta^{5+} , etc. In relation to other ruthenates, the 2:1 B-site ordering in $\text{Sr}_3\text{CaRu}_2\text{O}_9$ is intermediate between the all-ruthenium ferromagnetic SrRuO_3 ¹ and the 1:1 ordered antiferromagnetic Sr_2YRuO_6 .¹⁶ Work is in progress to demonstrate that, in general, we expect a number of homeotypic ruthenates with interesting magnetic and electronic properties to exist based on A- and B-site substitutions.^{17,18}

Acknowledgment. We gratefully acknowledge support from the National Science Foundation, Solid State Chemistry (Award No. DMR-9727516) and the use of the Central Facilities supported by the MRSEC program of the NSF (Grant DMR-0076097) at the Materials Research Center of Northwestern University. The work at IPNS was supported by DOE W-31-109-ENG-38. J.T.R. is supported by a National Science Foundation graduate research fellowship. J.T.R. thanks Takashi Saito, Dr. M. Azuma, and Professor M. Takano for useful discussions while a participant in the 2000 Summer Program in Japan supported by Monbusho and NSF.

Supporting Information Available: Tables listing detailed crystallographic data, atomic positions, bond lengths and selected bond angles based on the Rietveld refinement of the powder neutron diffraction data of $\text{Sr}_3\text{CaRu}_2\text{O}_9$; an indexed PXD profile and electron diffraction micrographs of $\text{Sr}_3\text{CaRu}_2\text{O}_9$ (PDF). This material is available free of charge via the Internet at <http://pubs.acs.org>.

References

- (1) Kanbayashi, A. *J. Phys. Soc. Jpn.* **1976**, *41*, 1876.
- (2) Longo, J. M.; Raccach, P. M.; Goodenough, J. B. *J. Appl. Phys.* **1968**, *39*, 1327.
- (3) He, T.; Cava, R. J. *J. Phys. Condens. Matter* **2001**, *13*, 8347.
- (4) Maeno, Y.; Hashimoto, H.; Yoshida, K.; Nishizaki, S.; Fujita T.; Bednorz, J. G.; Lichtenberg, F. *Nature* **1994**, *372*, 532.
- (5) Bernhard, C.; Tallon, J. L.; Niedermayer, Ch.; Blasius, Th.; Golinik, A.; Brücher, E.; Kremer, R. K.; Noakes, D. R.; Stronach, C. E.; Ansaldo, E. *J. Phys. Rev. B* **1999**, *59*, 14, 099.
- (6) Butera, A.; Fainstein, A.; Winkler, E.; Tallon, J. *Phys. Rev. B* **2001**, *63*, 54, 442.
- (7) Cava, R. J. *J. Mater. Chem.* **2001**, *11*, 54.
- (8) Galasso, F.; Pyle, J. *Inorg. Chem.* **1963**, *2*, 482.
- (9) Time-of-flight (TOF) powder neutron diffraction data were collected at room temperature using the special environment powder diffractometer at the Intense Pulsed Neutron Source at Argonne National Lab. Diffraction data were collected on all banks, but only the data from the high-resolution backscatter bank were used in the final analysis. The structural model was refined via the Rietveld method using the General Structure Analysis System (GSAS) software package (Larson, A. C.; Von Dreele, R. B. *General Structure Analysis System (GSAS)*; Los Alamos National Laboratory Report LAUR 86-748, 1994) and led to $R_p = 4.32\%$, $R_{wp} = 6.82\%$, $R_{exp} = 4.07\%$, $\chi^2 = 2.84$.
- (10) Anderson, M. T.; Vaughney, J. T.; Poeppelmeier, K. R. *Chem. Mater.* **1993**, *5*, 151.
- (11) Glazer, A. M. *Acta Crystallogr.* **1972**, *B28*, 3384.
- (12) Hervieu, M.; Studer, F.; Raveau, B. *J. Solid State Chem.* **1977**, *22*, 273.
- (13) Levin, I.; Bendersky, L. A.; Cline, J. P.; Roth, R. S.; Vanderah, T. A. *J. Solid State Chem.* **2000**, *150*, 43.
- (14) Nakatsuji, S.; Ando, T.; Mao, Z.; Maeno, Y. *Physica C* **1999**, *261*, 949.
- (15) Dussarrat, C.; Fompeyrine, J.; Darriet, J. *Eur. J. Solid State Inorg. Chem.* **1995**, *32*, 3.
- (16) Battle, P. D.; Macklin, W. J. *J. Solid State Chem.* **1984**, *52*, 138.
- (17) Vander Griend, D. A.; Boudin, S.; Caignaert, V.; Poeppelmeier, K. R.; Wang, Y.; Dravid, Vinayak, P. D.; Azuma, M.; Takano, M.; Hu, Z.; Jorgensen, J. D. *J. Am. Chem. Soc.* **1999**, *121*, 4787.
- (18) Vander Griend, D. A.; Malo, S.; Wang, T. K.; Poeppelmeier, K. R. *J. Am. Chem. Soc.* **2000**, *122*, 7308. JA017586P